Eur. Phys. J. Plus (2018) **133**: 94
DOI 10.1140/epjp/i2018-11947-6

THE EUROPEAN PHYSICAL JOURNAL PLUS

Regular Article

Comparing the Caputo, Caputo-Fabrizio and Atangana-Baleanu derivative with fractional order: Fractional cubic isothermal auto-catalytic chemical system⋆

K.M. Saad[1,2,a]

[1] Department of Mathematics, Faculty of Arts and Sciences, Najran University, Najran, Saudi Arabia
[2] Department of Mathematics, Faculty of Applied Science, Taiz University, Taiz, Yemen

Received: 1 November 2017 / Revised: 16 January 2018
Published online: 7 March 2018 – © Società Italiana di Fisica / Springer-Verlag 2018

Abstract. In this work we extend the standard model for a cubic isothermal auto-catalytic chemical system (CIACS) to a new model of a fractional cubic isothermal auto-catalytic chemical system (FCIACS) based on Caputo (C), Caputo-Fabrizio (CF) and Atangana-Baleanu in the Liouville-Caputo sense (ABC) fractional time derivatives, respectively. We present approximate solutions for these extended models using the q-homotopy analysis transform method (q-HATM). We solve the FCIACS with the C derivative and compare our results with those obtained using the CF and ABC derivatives. The ranges of convergence of the solutions are found and the optimal values of h, the auxiliary parameter, are derived. Finally, these solutions are compared with numerical solutions of the various models obtained using finite differences and excellent agreement is found.

1 Introduction

Two chemicals, which we label A and B, reacting through a mechanism known as cubic auto-catalysis are governed by the chemical reaction equation [1, 2]

$$A + 2B \rightarrow 3B, \quad \text{rate} \quad r_1[A][B]^2. \tag{1}$$

The product B then produces the product C through the linear decay

$$B \rightarrow C, \quad \text{rate} \quad r_2[B]. \tag{2}$$

Here r_i, $i = 1, 2$, are the reaction rate constants and A and B are the concentrations of the two chemicals, measured in moles. C is an inert product of the reaction. The chemical B is known as the auto-catalyst since it catalyses its own production. The greater the concentration of B, the faster it is produced by the reaction (1). If these two chemicals A and B then react in a long thin tube, so that their concentrations only vary in the ς direction along the tube, the main physical processes that act, in the absence of any underlying fluid flow, are chemical reaction and one dimensional diffusion. Under these assumptions the equation governing the chemical reaction (1) is the reaction-diffusion system

$$D_\tau u = d_1 \frac{\partial^2 u}{\partial \varsigma^2} - r_1 u v^2 \tag{3}$$

and

$$D_\tau v = d_2 \frac{\partial^2 v}{\partial \varsigma^2} + r_1 u v^2 - r_2 v. \tag{4}$$

⋆ Focus Point on "Modelling Complex Real-World Problems with Fractal and New Trends of Fractional Differentiation" edited by A. Atangana, Z. Hammouch, G. Mophou, K.M. Owolabi.

[a] e-mail: `khaledma_sd@hotmail.com`

Here, d_1 and d_2 are the diffusivity constants diffusivity of the chemicals. This system can be set in the non-dimensional form

$$D_\tau u = \frac{\partial^2 u}{\partial \varsigma^2} - uv^2 \tag{5}$$

and

$$D_\tau v = \frac{\partial^2 v}{\partial \varsigma^2} + uv^2 - kv. \tag{6}$$

Here τ is the dimensional time and the dimensionless constant k gives the strength of the auto-catalyst decay. If we now replace the time derivatives by fractional time derivatives, the system (5)-(6) becomes

$$D_\tau^\beta u = \frac{\partial^2 u}{\partial \varsigma^2} - uv^2 \tag{7}$$

and

$$D_\tau^\beta v = \frac{\partial^2 v}{\partial \varsigma^2} - kv + uv^2, \quad 0 < \beta \leq 1. \tag{8}$$

The boundary conditions for the model system are

$$u(0,t) = u(L,t) = 1, \qquad v(0,t) = v(L,t) = 0. \tag{9}$$

We solved this system without decay, *i.e.* $k = 0$, using the q-homotopy analysis method, the homotopy analysis transform method, the variational iteration method and the Adomian decomposition method in Caputo fractional derivatives [3].

Caputo and Fabrizio presented a new fractional differential operator that has the advantage of a kernel which is non-singular. This new operator has attracted the attention of many researchers, with this operator being applied to many model equations [4–10]. However, this operator has a major disadvantage: it is non-local since the associated integral is not a fractional operator. To overcome this disadvantage, Atangana and Baleanu introduced a new fractional operator in the Caputo and Riemann-Liouville sense [11], based on the Mittag-Leffler function. This operator has also attracted attention and has been applied to study a number of physical problems. Results for the derivatives of all the operators and their properties that used in this work have been proved previously [11–15]. Also, more recently, definitions of fractional derivatives involving the kernels of the Mittag-Leffler function have been proposed. Xia [16] structured nonlinear, local, fractional ODEs by means of a family of special functions via the Mittag-Leffler function defined on Cantor sets. In [17–23] these new general fractional derivatives were addressed using kernels of extended Mittag-Leffler–type functions.

The main goal of this paper is to obtain approximate solutions of the FCIACS system (7) and (8) by applying the C, CF and ABC operators using q-HATM. The present paper is organized as follows. The second section is devoted to the basic idea of the q-HATM and its application to (7)-(8) when $\beta = 1$. The third section is devoted to the computation of q-HATM solutions using the C, CF and ABC operators. The fourth section is devoted to the discussion of the numerical results. In the last section, conclusions are presented.

2 q-HATM solution when $\beta = 1$

In this section we apply the q-HATM to the FCIACS system (7) and (8) as in [24, 25]. We take the initial conditions to satisfy the boundary conditions, namely

$$u(\varsigma, 0) = 1 - \sum_{n=1}^{\infty} a \cos(0.5(L - 2\varsigma)\lambda_n) \sin(\lambda L/2) \tag{10}$$

and

$$v(\varsigma, 0) = \sum_{n=1}^{\infty} b \cos(0.5(L - 2\varsigma)\lambda_n) \sin(\lambda L/2), \tag{11}$$

where $\lambda_n = n\pi/L$. The q-HTAM is based on the continuous mapping [24–34]

$$u(\varsigma, \tau) \to \phi(\varsigma, \tau; q), \qquad v(\varsigma, \tau) \to \psi(\varsigma, \tau; q),$$

such that, as the embedding parameter q increases from 0 to $1/n$, $\phi(\varsigma, \tau; q)$ and $\psi(\varsigma, \tau; q)$ vary from the initial iterate to the exact solution.

We now define the nonlinear operators

$$\mathcal{N}(\phi(\varsigma,\tau;q)) = \mathcal{L}\left(\phi(\varsigma,\tau;q)\right) - \frac{1}{s}u(\varsigma,0) + \frac{1}{s}\mathcal{L}\left(-\phi_{\varsigma\varsigma}(\varsigma,\tau;q) + \phi(\varsigma,\tau;q)\psi^2(\varsigma,\tau;q)\right),$$
$$\mathcal{M}(\psi(\varsigma,\tau;q)) = \mathcal{L}\left(\psi(\varsigma,\tau;q)\right) - \frac{1}{s}v(\varsigma,0) + \frac{1}{s}\mathcal{L}\left(-\psi_{\varsigma\varsigma}(\varsigma,\tau;q) + k\psi(\varsigma,\tau;q) - \phi(\varsigma,\tau;q)\psi^2(\varsigma,\tau;q)\right).$$

Next, we develop a set of equations using the embedding parameter q

$$(1-nq)\mathcal{L}(\phi(\varsigma,\tau;q) - u_0(\varsigma,\tau)) = qhH(\varsigma,\tau)\mathcal{N}(\phi(\varsigma,\tau;q)),$$
$$(1-nq)\mathcal{L}(\psi(\varsigma,\tau;q) - v_0(\varsigma,\tau)) = qhH(\varsigma,\tau)\mathcal{M}(\psi(\varsigma,\tau;q)),$$

with the initial conditions $\phi(\varsigma,0;q) = u_0(\varsigma,0)$ and $\psi(\varsigma,0;q) = v_0(\varsigma,0)$. Here, $h \neq 0$ and $H(\varsigma,\tau) \neq 0$ are the auxiliary parameter and the auxiliary function, respectively. We expand $\phi(\varsigma,\tau;q)$ and $\psi(\varsigma,\tau;q)$ in series form by employing the Taylor theorem with respect to q to obtain

$$\phi(\varsigma,\tau;q) = u_0(\varsigma,\tau) + \sum_{m=1}^{\infty} u_m(\varsigma,\tau)q^m \tag{12}$$

and

$$\psi(\varsigma,\tau;q) = v_0(\varsigma,\tau) + \sum_{m=1}^{\infty} v_m(\varsigma,\tau)q^m, \tag{13}$$

where

$$u_m(\varsigma,\tau) = \frac{1}{m!}\frac{\partial^m \phi(\varsigma,\tau;q)}{\partial q^m}\bigg|_{q=0}$$

and

$$v_m(\varsigma,\tau) = \frac{1}{m!}\frac{\partial^m \psi(\varsigma,\tau;q)}{\partial q^m}\bigg|_{q=0}.$$

If we substitute $q = 1/n$ into (12)-(13), the series becomes

$$u(\varsigma,\tau) = u_0(\varsigma,\tau) + \sum_{m=1}^{\infty} u_m(\varsigma,\tau)\left(\frac{1}{n}\right)^m$$

and

$$v(\varsigma,\tau) = v_0(\varsigma,\tau) + \sum_{m=1}^{\infty} v_m(\varsigma,\tau)\left(\frac{1}{n}\right)^m.$$

Now, we construct the m-th–order deformation equation [24,25] as follows:

$$\mathcal{L}(u_m(\varsigma,\tau) - \mathcal{X}_m u_{(m-1)}(\varsigma,\tau)) = hH(\varsigma,\tau)R_1((\vec{u}_{(m-1)},\vec{v}_{(m-1)})),$$
$$\mathcal{L}(v_m(\varsigma,\tau) - \mathcal{X}_m v_{(m-1)}(\varsigma,\tau)) = hH(\varsigma,\tau)R_2((\vec{u}_{(m-1)},\vec{v}_{(m-1)})),$$

with the initial conditions $u_m(\varsigma,0) = 0$ and $v_m(\varsigma,0) = 0$, $m > 1$. We have set

$$R_1(\vec{u}_{(m-1)},\vec{v}_{(m-1)}) = \mathcal{L}\left(u_{(m-1)}(\varsigma,\tau)\right) - \frac{1}{s}u(\varsigma,0)\left(1 - \frac{\mathcal{X}_m}{n}\right) + \frac{1}{s}\mathcal{L}\left(-u_{(m-1),\varsigma\varsigma}(\varsigma,\tau) + u_{(m-1)}(\varsigma,\tau)v^2_{(m-1)}(\varsigma,\tau)\right)$$

and

$$R_2(\vec{u}_{(m-1)},\vec{v}_{(m-1)}) = \mathcal{L}\left(v_{(m-1)}(\varsigma,\tau)\right) - \frac{1}{s}v(\varsigma,0)\left(1 - \frac{\mathcal{X}_m}{n}\right) + \frac{1}{s}\mathcal{L}\left(-v_{(m-1),\varsigma\varsigma}(\varsigma,\tau) - v_{(m-1)}(\varsigma,\tau)v^2_{(m-1)}(\varsigma,\tau) + kv_{(m-1)}(\varsigma,\tau)\right),$$

with $\mathcal{L}$ denoting the Laplace transform. Taking the inverse Laplace transform gives

$$u_m = \mathcal{X}_m u_{(m-1)} + h\mathcal{L}^{-1}R_1((\vec{u}_{(m-1)},\vec{v}_{(m-1)})) \tag{14}$$

and

$$v_m = \mathcal{X}_m v_{(m-1)} + h\mathcal{L}^{-1}R_2((\vec{u}_{(m-1)},\vec{v}_{(m-1)})). \tag{15}$$

3 New q-HATM solution

In this section we apply the q-HATM to solve the FCIACS system (7) and (8) using the C, CF and ABC operators, respectively.

3.1 q-HATM solution via the Caputo fractional time derivative

The FCIACS can be replaced by its equivalent FCIACS with the C fractional time derivative by replacing $D_\tau^\beta u$ and $D_\tau^\beta v$ by ${}_0^{\mathrm{C}}D_\tau^\beta u$ and ${}_0^{\mathrm{C}}D_\tau^\beta v$, respectively, where $0 < \beta \leq 1$. We then obtain the C fractional time derivative equations

$$ {}_0^{\mathrm{C}}D_\tau^\beta u(\varsigma,\tau) - u_{\varsigma\varsigma}(\varsigma,\tau) + u(\varsigma,\tau)v^2(\varsigma,\tau) = 0 \tag{16}$$

and

$$ {}_0^{\mathrm{C}}D_\tau^\beta v(\varsigma,\tau) - v_{\varsigma\varsigma}(\varsigma,\tau) - u(\varsigma,\tau)v^2(\varsigma,\tau) + kv(\varsigma,\tau) = 0, \tag{17}$$

where

$$ {}_0^{\mathrm{C}}D_\tau^\beta u = \frac{1}{\Gamma(n-\beta)}\int_0^\tau (\tau - t)^{n-\beta-1}D^n u(\varsigma,t)\mathrm{d}t$$

and

$$ {}_0^{\mathrm{C}}D_\tau^\beta v = \frac{1}{\Gamma(n-\beta)}\int_0^\tau (\tau - t)^{n-\beta-1}D^n v(\varsigma,t)\mathrm{d}t.$$

Taking the Laplace transform of (16)-(17), we obtain

$$ s^\beta\mathcal{L}(u(\varsigma,\tau)) - s^{\beta-1}u(\varsigma,0) = \mathcal{L}\left(u_{\varsigma\varsigma}(\varsigma,\tau) - u(\varsigma,\tau)v^2(\varsigma,\tau)\right) \tag{18}$$

and

$$ s^\beta\mathcal{L}(v(\varsigma,\tau)) - s^{\beta-1}v(\varsigma,0) = \mathcal{L}\left(v_{\varsigma\varsigma}(\varsigma,\tau) + u(\varsigma,\tau)v^2(\varsigma,\tau) - kv(\varsigma,\tau)\right). \tag{19}$$

By the same procedure as in sect. 2 the m-th approximation solution is then given by

$$ u_m = \mathcal{X}_m u_{(m-1)} + h\mathcal{L}^{-1}R_1^{\mathrm{C}}((\vec{u}_{(m-1)}, \vec{v}_{(m-1)})) \tag{20}$$

and

$$ v_m = \mathcal{X}_m v_{(m-1)} + h\mathcal{L}^{-1}R_2^{\mathrm{C}}((\vec{u}_{(m-1)}, \vec{v}_{(m-1)})), \tag{21}$$

where

$$ \begin{aligned} R_1^{\mathrm{C}}\left(\vec{u}_{(m-1)}, \vec{v}_{(m-1)}\right) = {} & \mathcal{L}\left(u_{(m-1)}(\varsigma,\tau)\right) - \frac{1}{s}u(\varsigma,0)\left(1 - \frac{\mathcal{X}_m}{n}\right) \\ & + \frac{1}{s^\beta}\mathcal{L}\left(-u_{(m-1),\varsigma\varsigma}(\varsigma,\tau) + u_{(m-1)}(\varsigma,\tau)v_{(m-1)}^2(\varsigma,\tau)\right) \end{aligned}$$

and

$$ \begin{aligned} R_2^{\mathrm{C}}\left(\vec{u}_{(m-1)}, \vec{v}_{(m-1)}\right) = {} & \mathcal{L}_{(m-1)}\left(v_{(m-1)}(\varsigma,\tau)\right) - \frac{1}{s}v(\varsigma,0)\left(1 - \frac{\mathcal{X}_m}{n}\right) \\ & + \frac{1}{s^\beta}\mathcal{L}\left(-v_{(m-1),\varsigma\varsigma}(\varsigma,\tau) - v_{(m-1)}(\varsigma,\tau)v_{(m-1)}^2(\varsigma,\tau) + kv_{(m-1)}(\varsigma,\tau)\right). \end{aligned}$$

3.2 q-HAM solution via the Caputo-Fabrizio fractional time derivative

The FCIACS system (7) and (8) can be replaced by its equivalent FCIACS with a CF fractional time derivative by replacing $D_\tau^\beta u$ and $D_\tau^\beta v$ by ${}_0^{\mathrm{CF}}D_\tau^\beta u$ and ${}_0^{\mathrm{CF}}D_\tau^\beta v$, respectively, where $0 < \beta \leq 1$. We then obtain the CF fractional time derivative system [13,15]

$$ {}_0^{\mathrm{CF}}D_\tau^\beta u(\varsigma,\tau) - u_{\varsigma\varsigma}(\varsigma,\tau) + u(\varsigma,\tau)v^2(\varsigma,\tau) = 0 \tag{22}$$

and

$$ {}_0^{\mathrm{CF}}D_\tau^\beta v(\varsigma,\tau) - v_{\varsigma\varsigma}(\varsigma,\tau) - u(\varsigma,\tau)v^2(\varsigma,\tau) + kv(\varsigma,\tau) = 0. \tag{23}$$

${}_{0}^{\mathrm{CF}}D_{\tau}^{\beta}$ is known as the CF fractional time derivative of order β and is given by

$$ {}_{0}^{\mathrm{CF}}D_{\tau}^{\beta}u(\varsigma,\tau)=\frac{M(\beta)}{1-\beta}\int_{0}^{\tau}\exp\left(\frac{-\beta(\tau-t)}{1-\beta}\right)Du(\varsigma,t)\mathrm{d}t $$

and

$$ {}_{0}^{\mathrm{CF}}D_{\tau}^{\beta}v(\varsigma,\tau)=\frac{M(\beta)}{1-\beta}\int_{0}^{\tau}\exp\left(\frac{-\beta(\tau-t)}{1-\beta}\right)Dv(\varsigma,t)\mathrm{d}t, $$

where $M(\beta)$ is a normalization function, such that $M(0)=M(1)=1$.

Taking the Laplace transform of (22)-(23), we obtain

$$ \frac{M(\beta)(s\mathcal{L}(u(\varsigma,\tau))-u(\varsigma,0))}{(s+\beta(1-s))}=\mathcal{L}\left(u_{\varsigma\varsigma}(\varsigma,\tau)-u(\varsigma,\tau)v^{2}(\varsigma,\tau)\right) \tag{24} $$

and

$$ \frac{M(\beta)(s\mathcal{L}(v(\varsigma,\tau))-v(\varsigma,0))}{(s+\beta(1-s))}=\mathcal{L}\left(v_{\varsigma\varsigma}(\varsigma,\tau)+u(\varsigma,\tau)v^{2}(\varsigma,\tau)-kv(\varsigma,\tau)\right). \tag{25} $$

By following the same procedure as in sect. 2, we hence obtain the iterates

$$ u_{m}=\mathcal{X}_{m}u_{(m-1)}+h\mathcal{L}^{-1}R_{1}^{\mathrm{CF}}((\vec{u}_{(m-1)},\vec{v}_{(m-1)})) \tag{26} $$

and

$$ v_{m}=\mathcal{X}_{m}v_{(m-1)}+h\mathcal{L}^{-1}R_{2}^{\mathrm{CF}}((\vec{u}_{(m-1)},\vec{v}_{(m-1)})). \tag{27} $$

Here

$$ \begin{aligned} R_{1}^{\mathrm{CF}}\left(\vec{u}_{(m-1)},\vec{v}_{(m-1)}\right)=&\,\mathcal{L}\left(u_{(m-1)}(\varsigma,\tau)\right)-\frac{1}{s}u(\varsigma,0)\left(1-\frac{\mathcal{X}_{m}}{n}\right)\\ &+\frac{\beta(1-s)+s}{sM(\beta)}\mathcal{L}\left(-u_{(m-1),\varsigma\varsigma}(\varsigma,\tau)+u_{(m-1)}(\varsigma,\tau)v_{(m-1)}^{2}(\varsigma,\tau)\right) \end{aligned} $$

and

$$ \begin{aligned} R_{2}^{\mathrm{CF}}\left(\vec{u}_{(m-1)},\vec{v}_{(m-1)}\right)=&\,\mathcal{L}_{(m-1)}\left(v_{(m-1)}(\varsigma,\tau)\right)-\frac{1}{s}v(\varsigma,0)\left(1-\frac{\mathcal{X}_{m}}{n}\right)\\ &+\frac{\beta(1-s)+s}{sM(\beta)}\mathcal{L}\left(-v_{(m-1),\varsigma\varsigma}(\varsigma,\tau)-v_{(m-1)}(\varsigma,\tau)v_{(m-1)}^{2}(\varsigma,\tau)+kv(\varsigma,\tau)\right). \end{aligned} $$

3.3 q-HAM solution via the Atangana-Baleanu fractional time derivative

The FCIACS system ${}_{0}^{\mathrm{CF}}D_{\tau}^{\beta}u$ can be replaced by its equivalent FCIACS system with ABC fractional time derivatives by replacing $D_{\tau}^{\beta}u$ and $D_{\tau}^{\beta}v$ by ${}_{0}^{\mathrm{ABC}}D_{\tau}^{\beta}u$ and ${}_{0}^{\mathrm{ABC}}D_{\tau}^{\beta}v$, respectively, where $0<\beta\leq 1$. We then obtain the ABC fractional time derivative system [35,36]

$$ {}_{0}^{\mathrm{ABC}}D_{\tau}^{\beta}u(\varsigma,\tau)-u_{\varsigma\varsigma}(\varsigma,\tau)+u(\varsigma,\tau)v^{2}(\varsigma,\tau)=0 \tag{28} $$

and

$$ {}_{0}^{\mathrm{ABC}}D_{\tau}^{\beta}v(\varsigma,\tau)-v_{\varsigma\varsigma}(\varsigma,\tau)-u(\varsigma,\tau)v^{2}(\varsigma,\tau)+kv(\varsigma,\tau)=0. \tag{29} $$

Here, ${}_{0}^{\mathrm{ABC}}D_{\tau}^{\beta}(\cdot)$ is known as the ABC fractional time derivative of order β in the Liouville-Caputo sense, given by

$$ {}_{0}^{\mathrm{ABC}}D_{\tau}^{\beta}u(\varsigma,\tau)=\frac{M(\beta)}{1-\beta}\int_{0}^{\tau}E_{\beta}\left(\frac{-\beta(\tau-t)}{1-\beta}\right)Du(\varsigma,t)\mathrm{d}t $$

and

$$ {}_{0}^{\mathrm{ABC}}D_{\tau}^{\beta}v(\varsigma,\tau)=\frac{M(\beta)}{1-\beta}\int_{0}^{\tau}E_{\beta}\left(\frac{-\beta(\tau-t)}{1-\beta}\right)Dv(\varsigma,t)\mathrm{d}t, $$

where

$$ E_{\beta}(z)=\sum_{k=0}^{\infty}\frac{z^{k}}{\Gamma(\beta k+1)} \tag{30} $$

is the Mittag-Leffler function and $M(\beta)$ is a normalization function. It has the same properties as in the Liouville-Caputo and Caputo-Fabrizio cases. Taking the Laplace transform of (28)-(29), we obtain [35, 36]

$$\frac{M(\beta)(\mathcal{L}(u(\varsigma,\tau))s^{\beta}-u(\varsigma,0)s^{\beta-1})}{(1-\beta)(\frac{\beta}{1-\beta}+s^{\beta})}=\mathcal{L}\left(u_{\varsigma\varsigma}(\varsigma,\tau)-u(\varsigma,\tau)v^{2}(\varsigma,\tau)\right) \tag{31}$$

and

$$\frac{M(\beta)(\mathcal{L}(v(\varsigma,\tau))s^{\beta}-v(\varsigma,0)s^{\beta-1})}{(1-\beta)(\frac{\beta}{1-\beta}+s^{\beta})}=\mathcal{L}\left(v_{\varsigma\varsigma}(\varsigma,\tau)+u(\varsigma,\tau)v^{2}(\varsigma,\tau)-kv(\varsigma,\tau)\right). \tag{32}$$

By following the same procedure as in sect. 2, we have

$$u_m=\mathcal{X}_m u_{(m-1)}+h\mathcal{L}^{-1}R_1^{\mathrm{ABC}}\left((\vec{u}_{(m-1)},\vec{v}_{(m-1)})\right) \tag{33}$$

and

$$v_m=\mathcal{X}_m v_{(m-1)}+h\mathcal{L}^{-1}R_2^{\mathrm{ABC}}\left((\vec{u}_{(m-1)},\vec{v}_{(m-1)})\right), \tag{34}$$

where

$$\begin{aligned}R_1^{\mathrm{ABC}}(\vec{u}_{(m-1)},\vec{v}_{(m-1)})&=\mathcal{L}\left(u_{(m-1)}(\varsigma,\tau)\right)-\frac{1}{s}u(\varsigma,0)\left(1-\frac{\mathcal{X}_m}{n}\right)\\&\quad+\frac{s^{-\beta-1}(\beta s^{\beta+1}-s^{\beta+1}-\beta s)}{M(\beta)}\\&\quad\times\mathcal{L}\left(-u_{(m-1),\varsigma\varsigma}(\varsigma,\tau)+u_{(m-1)}(\varsigma,\tau)v^{2}_{(m-1)}(\varsigma,\tau)\right)\end{aligned} \tag{35}$$

and

$$\begin{aligned}R_2^{\mathrm{ABC}}(\vec{u}_{(m-1)},\vec{v}_{(m-1)})&=\mathcal{L}_{(m-1)}\left(v_{(m-1)}(\varsigma,\tau)\right)-\frac{1}{s}v(\varsigma,0)\left(1-\frac{\mathcal{X}_m}{n}\right)\\&\quad+\frac{s^{-\beta-1}(\beta s^{\beta+1}-s^{\beta+1}-\beta s)}{M(\beta)}\\&\quad\times\mathcal{L}\left(-v_{(m-1),\varsigma\varsigma}(\varsigma,\tau)-v_{(m-1)}(\varsigma,\tau)v^{2}_{(m-1)}(\varsigma,\tau)+kv_{m-1}(\varsigma,\tau)\right).\end{aligned} \tag{36}$$

4 Numerical results

In this section we evaluate the first approximations based on the C, CF and ABC operators. We then explore the intervals of convergence given by the h-curves and the averaged residual error for the C, CF and ABC, respectively. Finally, we test the accuracy of the q-HATM for the C, CF and ABC operator equations by comparing the analytical results with numerical results obtained using the `NDSolve` of Mathematica, which is based on the finite difference method.

We take the initial approximation as

$$u_0(\varsigma,\tau)=u_0(\varsigma,0),\qquad v_0(\varsigma,\tau)=v_0(\varsigma,0). \tag{37}$$

For $m=1$, we hence obtain the first approximation as

$$u_1(\varsigma,\tau)=h\mathcal{L}^{-1}\left(\mathcal{L}\left(u_0(\varsigma,\tau)\right)-\frac{1}{s}u(\varsigma,0)\left(1-\frac{\mathcal{X}_m}{n}\right)+\Omega_i(s)\mathcal{L}\left(-u_{0,\varsigma\varsigma}(\varsigma,\tau)+u_0(\varsigma,\tau)v_0^2(\varsigma,\tau)\right)\right) \tag{38}$$

and

$$v_1(\varsigma,\tau)=h\mathcal{L}^{-1}\left(\mathcal{L}\left(v_0(\varsigma,\tau)\right)-\frac{1}{s}v(\varsigma,0)\left(1-\frac{\mathcal{X}_m}{n}\right)+\Omega_i(s)\mathcal{L}\left(-v_{0,\varsigma\varsigma}(\varsigma,\tau)+kv_0(\varsigma,\tau)-u_0(\varsigma,\tau)v_0^2(\varsigma,\tau)\right)\right), \tag{39}$$

for $i=1,2,3$. Now if we take

$$\Omega_1(s)=1/s^{\beta},\qquad \Omega_2(s)=\frac{(s+\beta(1-s))}{sM(\beta)},\qquad \Omega_3(s)=\frac{s^{-\beta-1}(\beta s^{\beta+1}-s^{\beta+1}-\beta s)}{M(\beta)}, \tag{40}$$

we can obtain the first approximation for the C, CF and ABC operator equations as

$$u_1(\varsigma,\tau) = f(\theta,\Theta) + \omega_i^{(\cdot)}(\tau,\beta)\left(aL^{-2}(88.83\cos(\Theta) - 9.87\cos(\theta)) + f(\theta,\Theta)(g(\theta))^2\right) \tag{41}$$

and

$$v_1(\varsigma,\tau) = g(\theta) + \omega_i^{(\cdot)}(\tau,\beta)\left(bL^{-2}(-88.83\cos(\Theta) + 9.87\cos(\theta)) + kg(\theta) - f(\theta,\Theta)g^2(\theta)\right), \tag{42}$$

where

$$f(\theta,\Theta) = 1 - a\cos(\theta) + a\cos(\Theta), \qquad g(\theta) = b\cos(\theta) - b\cos(\Theta),$$
$$\theta = 1.57(1 - 2\varsigma L^{-1}), \qquad \Theta = 4.71(1 - 2\varsigma L^{-1})$$

and

$$\omega_1^{\mathrm{C}}(\tau) = \frac{h\tau^\beta}{n\Gamma(\beta+1)},$$
$$\omega_2^{\mathrm{CF}}(\tau) = \frac{h}{nM(\beta)}(1-\beta+\beta\tau),$$
$$\omega_2^{\mathrm{ABC}}(\tau) = \frac{h}{nM(\beta)}\left(1-\beta+\frac{\beta\tau^\beta}{\Gamma(\beta+1)}\right).$$

By the same procedure we can evaluate further approximations. We therefore have q-HATM solutions for the C fractional time derivative equations (16)-(17), the CF fractional time derivative equations (22)-(23) and the ABC fractional time derivative equations (28)-(29) as

$$u(\varsigma,\tau) = u_0(\varsigma,\tau) + \sum_{i=1}^{m}\frac{u_i(\varsigma,\tau)}{n^i} \tag{43}$$

and

$$v(\varsigma,\tau) = v_0(\varsigma,\tau) + \sum_{i=1}^{m}\frac{v_i(\varsigma,\tau)}{n^i}. \tag{44}$$

To obtain the intervals of convergence of the q-HATM solutions, we plot the h-curves for 6 terms of the q-HATM solutions for the C fractional time derivative equations (16)-(17), the CF fractional time derivative equations (22)-(23) and the ABC fractional time derivative equations (28)-(29), respectively. In figs. 1–4 we plot $u_\tau(\varsigma,0)$ and $v_\tau(\varsigma,0)$ against h. These figures represent the h-curves for the C, CF and ABC operator equations, respectively, at $k=0.01$, $L=100$, $\varsigma=3$, $a=0.001$ and $b=0.001$ for different values of β and n. From these figures, we note that the straight line that parallels the h-axis provides the region of convergence [30]. Also, the h curves at $\beta=1$ for the three operators coincide. We notice, however, that h-curve does not give the optimal value of the parameter h. So, we compute the optimal values of the convergence control parameter from the minimum of the averaged residual errors [25, 34, 37–46]

$$E_u(h) = \frac{1}{(N+1)(M+1)}\sum_{i=0}^{N}\sum_{j=0}^{M}\left[\mathcal{N}\left(\sum_{k=0}^{m}u_k\left(\frac{10i}{N},\frac{10j}{M}\right)\right)\right]^2 \tag{45}$$

and

$$E_v(h) = \frac{1}{(N+1)(M+1)}\sum_{i=0}^{N}\sum_{j=0}^{M}\left[\mathcal{M}\left(\sum_{k=0}^{m}v_k\left(\frac{10i}{N},\frac{10j}{M}\right)\right)\right]^2, \tag{46}$$

corresponding to the nonlinear algebraic equations

$$\frac{\mathrm{d}E_u(h)}{\mathrm{d}h} = 0 \quad \text{and} \quad \frac{\mathrm{d}E_v(h)}{\mathrm{d}h} = 0. \tag{47}$$

We show $E_u(h)$ and $E_v(h)$ in figs. 5–7 and in table 1 for the C, CF and ABC operator equations. Figures 5–7 and table 1 show that $E_u(h)$ and $E_v(h)$ for the 6-term q-HATM solutions using the C, CF and ABC operators, respectively. We have used the parameter values $N=10$ and $M=10$ with $k=0.01$, $L=10$, $a=0.001$ and $b=0.001$ in (45)-(46). We split table 1 into two sections, one for the optimal values of h_u and $E_u(h)$ and other for h_u and $E_u(h)$. We used the command `Minimize` of Mathematica and plotted the residual error against h to obtain the optimal values h.

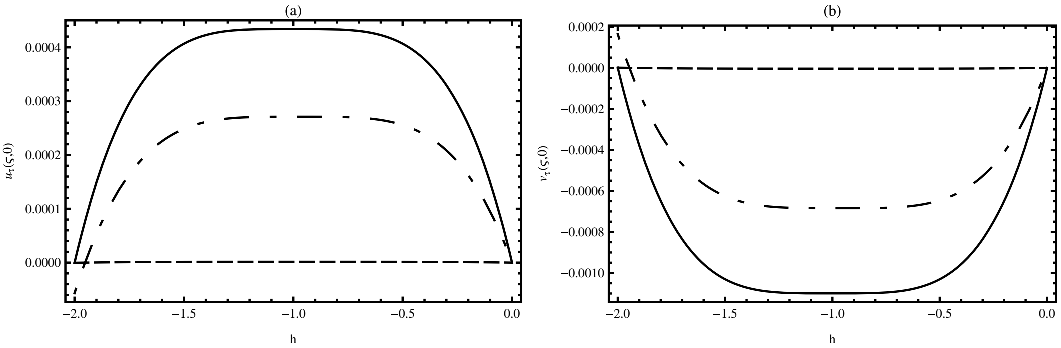

Fig. 1. Plotting the h-curves for 6 terms of q-HATM solutions with $\beta = 0.5$, $n = 1$, $\varsigma = 3$, $\tau = 0$, $k = 0.01$, $L = 100$, $a = 0.001$, $b = 0.001$. Dash-dotted line (C), dotted line (CF), and solid line (ABC).

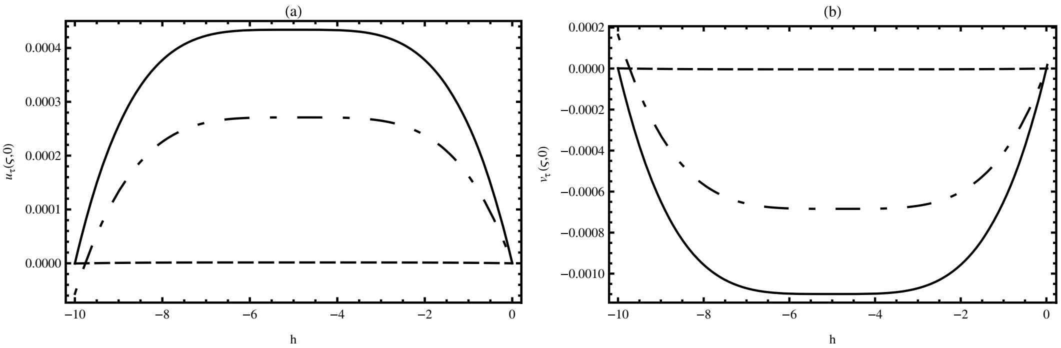

Fig. 2. Plotting the h-curves for 6 terms of q-HATM solutions with $\beta = 0.5$, $n = 5$, $\varsigma = 3$, $\tau = 0$, $k = 0.01$, $L = 100$, $a = 0.001$, $b = 0.001$. Dash-dotted line (C), dotted line (CF), and solid line (ABC).

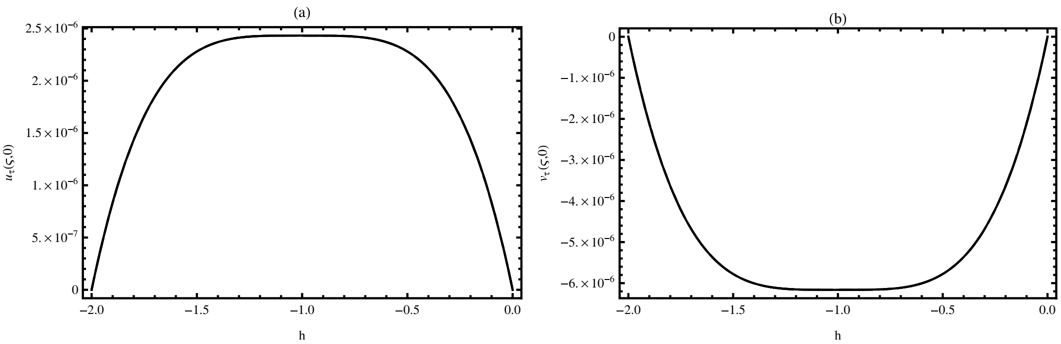

Fig. 3. Plotting the h-curves for 6 terms of q-HATM solutions with $\beta = 1$, $n = 1$, $\varsigma = 3$, $\tau = 0$, $k = 0.01$, $L = 100$, $a = 0.001$, $b = 0.001$. Dash-dotted line (C), dotted line (CF), and solid line (ABC).

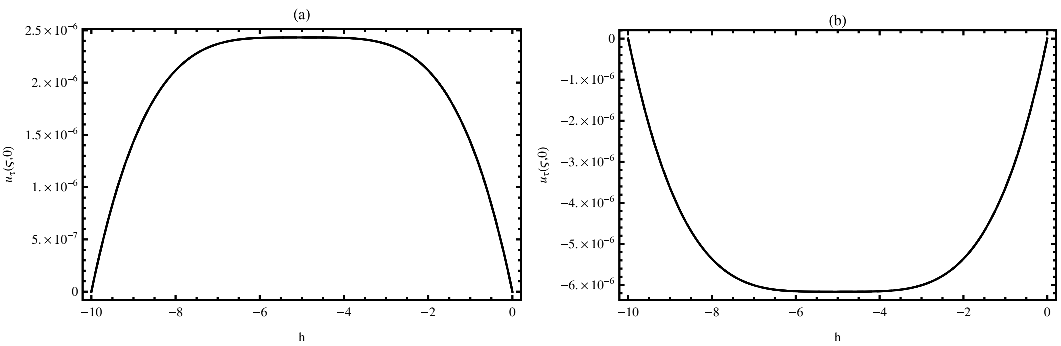

Fig. 4. Plotting the h-curves for 6 terms of q-HATM solutions with $\beta = 1$, $n = 5$, $\varsigma = 3$, $\tau = 0$, $k = 0.01$, $L = 100$, $a = 0.001$, $b = 0.001$. Dash-dotted line (C), dotted line (CF), and solid line (ABC).

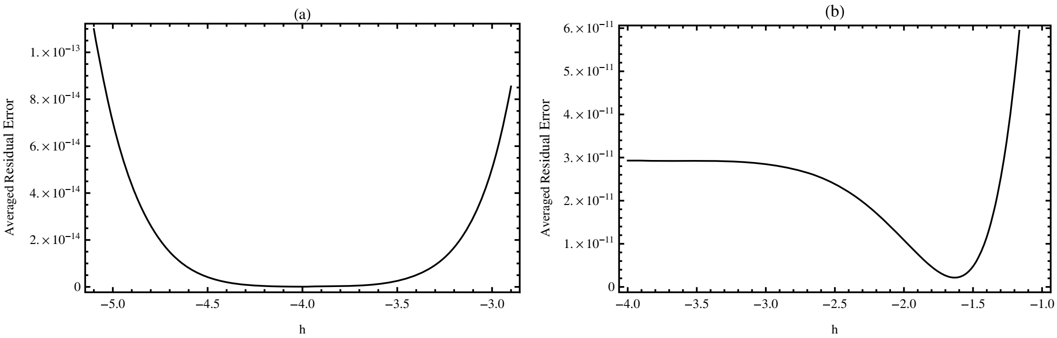

Fig. 5. Plotting the average residual error for 6 terms of q-HATM solutions with $\beta = 0.5$, $n = 5$, $\leq \varsigma \leq 10$, $0 \leq \tau \leq 10$, $k = 0.01$, $a = 0.001$, $b = 0.001$ for the C operator.

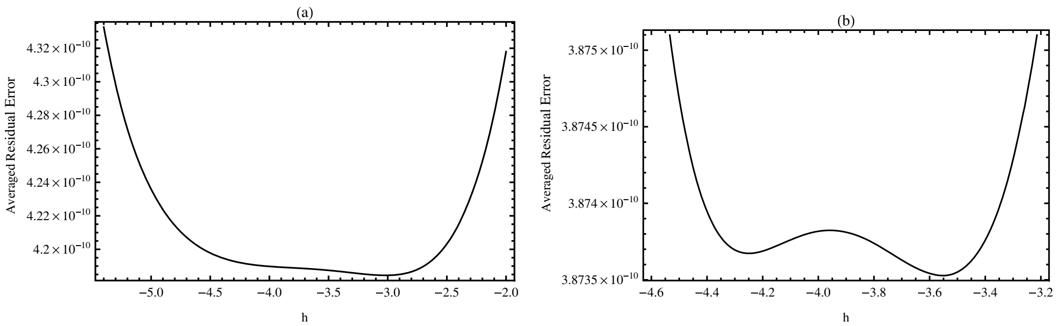

Fig. 6. Plotting the average residual error for 6 terms of q-HATM solutions with $\beta = 0.5$, $n = 5$, $\leq \varsigma \leq 10$, $0 \leq \tau \leq 10$, $k = 0.01$, $a = 0.001$, $b = 0.001$ for the CF operator.

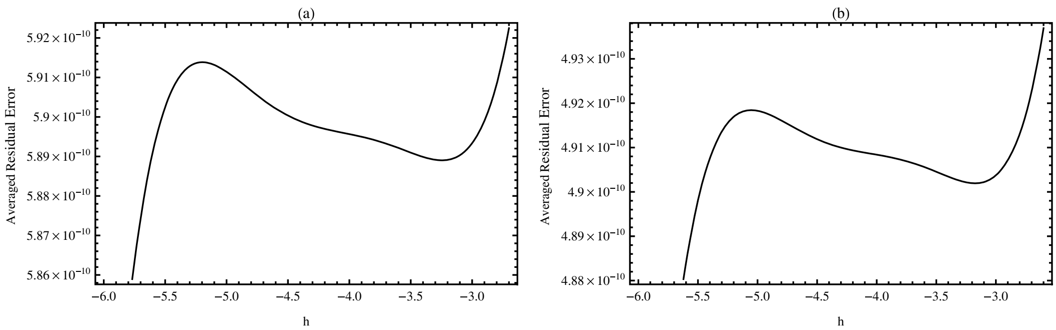

Fig. 7. Plotting the average residual error for 6 terms of q-HATM solutions with $\beta = 0.5$, $n = 5$, $0 \leq \varsigma \leq 10$, $0 \leq \tau \leq 10$, $k = 0.01$, $a = 0.001$, $b = 0.001$ for the ABC operator.

Table 1. The average residual error for 6 terms of q-HATM solutions with $\beta = 0.5$, $n = 5$, $0 \leq \varsigma \leq 10$, $0 \leq \tau \leq 10$, $k = 0.01$, $a = 0.001$, $b = 0.001$ using C, CF, and ABC operators, respectively.

Operators	Optimal value of h_u	Minimum of $E_u(h)$
C	-3.99021	8.65012×10^{-17}
CF	-3.01658	4.18446×10^{-10}
ABC	-3.2452	5.88902×10^{-10}

Operators	Optimal value of h_v	Minimum of $E_v(h)$
C	-1.6323	2.1557×10^{-12}
CF	-3.55406	3.87353×10^{-10}
ABC	-3.17425	4.90194×10^{-10}

Table 2. The absolute error of 6 terms of q-HATM solution (43) using C, CF and ABC operators with numerical solution by Mathematica at $\beta = 0.95$, $k = 0.01$, $\varsigma = 20$, $n = 5$, $a = 0.001$, $b = 0.001$.

τ	Error for C	Error for CF	Error for ABC
0	1.03529×10^{-8}	1.39257×10^{-7}	1.39257×10^{-7}
10	1.79961×10^{-4}	1.77823×10^{-4}	1.80382×10^{-4}
20	3.35654×10^{-4}	3.29769×10^{-4}	3.36600×10^{-4}
30	4.68161×10^{-4}	4.57944×10^{-4}	4.69612×10^{-4}
40	5.80085×10^{-4}	5.65189×10^{-4}	5.82026×10^{-4}
50	6.73774×10^{-4}	6.53966×10^{-4}	6.76194×10^{-4}
60	7.51785×10^{-4}	7.26895×10^{-4}	7.54673×10^{-4}
70	8.16269×10^{-4}	7.86171×10^{-4}	8.19616×10^{-4}
80	8.69044×10^{-4}	8.33644×10^{-4}	8.72842×10^{-4}
90	9.11737×10^{-4}	8.70963×10^{-4}	9.15977×10^{-4}
100	9.45882×10^{-4}	8.99678×10^{-4}	9.50555×10^{-4}

Table 3. The absolute error of 6 terms of q-HATM solution (44) using C, CF and ABC operators with numerical solution by Mathematica at $\beta = 0.95$, $k = 0.01$, $\varsigma = 20$, $n = 5$, $a = 0.001$, $b = 0.001$.

τ	Error for C	Error for CF	Error for ABC
0	1.03530×10^{-8}	1.39257×10^{-7}	1.3925691×10^{-7}
10	1.79961×10^{-4}	1.77823×10^{-4}	1.80382×10^{-4}
20	3.35654×10^{-4}	3.29769×10^{-4}	3.366×10^{-4}
30	4.68161×10^{-4}	4.57944×10^{-4}	4.69612×10^{-4}
40	5.80085×10^{-4}	5.65189×10^{-4}	5.82026×10^{-4}
50	6.73774×10^{-4}	6.53966×10^{-4}	6.76194×10^{-4}
60	7.51785×10^{-4}	7.26895×10^{-4}	7.54673×10^{-4}
70	8.16269×10^{-4}	7.86171×10^{-4}	8.19616×10^{-4}
80	8.69044×10^{-4}	8.33644×10^{-4}	8.72842×10^{-4}
90	9.11737×10^{-4}	8.70963×10^{-4}	9.15977×10^{-4}
100	9.45882×10^{-4}	8.99678×10^{-4}	9.50555×10^{-4}

From figs. 5–7 and table 1 we observe that the average residual error is of order $10^{-10} - 10^{-17}$. This observation shows that the q-HATM solutions for the C, CF and ABC operator equations converge rapidly.

We now compare the 6-term q-HATM solutions with numerical solutions of the C fractional time derivative equations (16)-(17), the CF fractional time derivative equations (22)-(23) and the ABC fractional time derivative equations (28)-(29), these numerical solutions obtained using Mathematica 9. These comparisons are shown in tables 2 and 3 and figs. 8 and 9. These tables and figures show the absolute error of the q-HATM solutions based on the numerical solutions with $\beta = 0.95$ and 1.0, respectively, with $n = 5$, $k = 0.01$, $L = 100$, $a = 0.001$, $b = 0.001$.

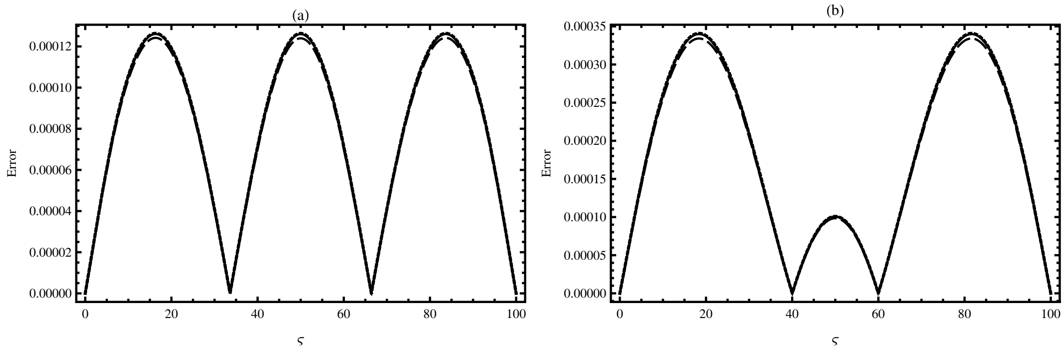

Fig. 8. Plotting the absolute error of 6 terms of q-HATM solutions (43) and (44), respectively, using C, CF and ABC operators with numerical solution by Mathematica at $\beta = 0.95$, $k = 0.01$, $\varsigma = 20$, $n = 5$, $a = 0.001$, $b = 0.001$. Dash-dotted line (C), dotted line (CF), and solid line (ABC). (a) $u(\varsigma, \tau)$ and (b) $v(\varsigma, \tau)$.

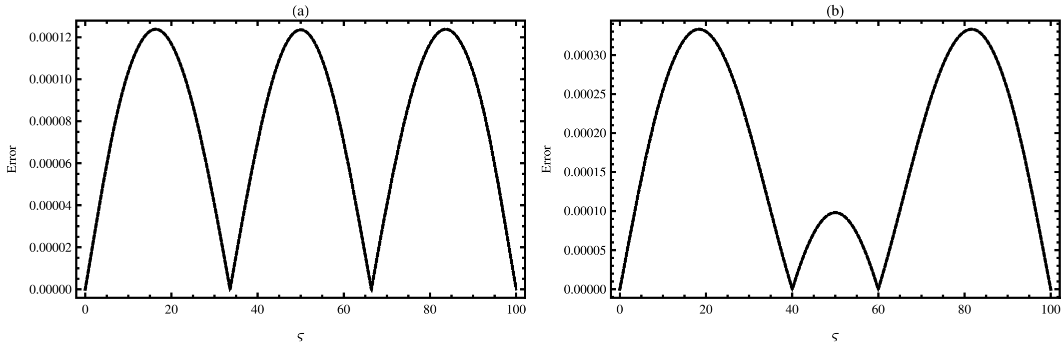

Fig. 9. Plotting the absolute error of 6 terms of q-HATM solutions (43) and (44), respectively, using C, CF and ABC operators with numerical solution by Mathematica at $\beta = 1$, $k = 0.01$, $\varsigma = 20$, $n = 5$, $a = 0.001$, $b = 0.001$. Dash-dotted line (C), dotted line (CF), and solid line (ABC). (a) $u(\varsigma, \tau)$ and (b) $v(\varsigma, \tau)$.

We observe from these tables and figures that the q-HATM solutions for all the operators are in excellent agreement with the results from Mathematica. In the case $\beta = 1$, the absolute errors are identical for all operators. This case shows that all the operators approach the classical system and solution when $\beta \to 1$.

5 Conclusions

In this paper the q-HATM was employed analytically to compute approximate solutions of the FCIACS system (7) and (8) using C, CF and ABC operator time derivatives. Therefore, CF and ABC were used in this paper to present alternative solutions of the FCIACS system. We compared these approximate solutions with numerical solutions and excellent agreement was found. Also, the interval of the convergence of the q-HATM and the optimal values of h were computed. The orders of the average residual error show that the approximations that have been calculated using the q-HATM with C, CF, and ABC have high accuracy.

I would like to thank Prof. Atangana Abdon, University of the Free State, South Africa for stimulating discussions during the preparation of this article and Prof. Noel Frederick Smyth, University of Edinburgh, United Kingdom for editing this article.

References

1. A.C. King, J. Billingham, S.R. Otto, *Differential Equations: Linear, Nonlinear, Ordinary, Partial* (Cambridge University Press, 2003).
2. Qi. Yuanwei, Zhu Yi, Commun. Comput. Phys. **19**, 1461 (2016).
3. K.M. Saad, Eman. H.F. AL-Sharif, *Comparative study of a cubic autocatalytic reaction via different analysis methods*, submitted to Discr. Contin. Dyn. Syst. Ser. S.
4. A. Alsaedi *et al.*, J. Funct. Spaces **2016**, 4626940 (2016).
5. A. Atangana, J.J. Nieto, Adv. Mech. Eng. (2015) https://doi.org/10.1177/1687814015613758.

6. A. Atangana, Appl. Math. Comput. **273**, 948 (2016).
7. A. Atangana, S.T.A. Badr, Entropy **17**, 4439 (2015).
8. A. Atangana, S.T.A. Badr, Adv. Mech. Eng. (2015) https://doi.org/10.1177/1687814015591937.
9. A. Atangana, S.T.A. Badr, Arab. J. Geosci. **9**, 8 (2016).
10. J.F. Gomez-Aguilar *et al.*, Entropy **17**, 6289 (2015).
11. A. Atangana, D. Baleanu, Therm. Sci **20**, 763 (2016).
12. A. Atangana, D. Baleanu. arXiv:1602.03408 (2016).
13. M. Caputo, M. Fabrizio, Progr. Fract. Differ. Appl. **1**, 73 (2015).
14. M. Caputo, M. Fabrizio, Progr. Fract. Differ. Appl. **2**, 1 (2016).
15. J.J. Nieto, J. Losada, Progr. Fract. Differ. Appl. **2**, 87 (2015).
16. X.-J. Yang, F. Gao, H.M. Srivastava, Fractals **25**, 1740002 (2017).
17. F. Gao, Therm. Sci. **21**, S11 (2017).
18. X.-J. Yang, Therm. Sci. **21**, 1161 (2017).
19. X.-J. Yang, Therm. Sci. **21**, S317 (2017).
20. X.-J. Yang, Rom. Rep. Phys. **69**, 118 (2017).
21. X.-J. Yang, J.A.T. Machado, D. Baleanu, Rom. Rep. Phys. **69**, 115 (2017).
22. X.-J. Yang, H.M. Srivastava, J.A.T. Machado, Therm. Sci. **20**, 753 (2017).
23. X.-J. Yang, H.M. Srivastava, D.F.M. Torres, A. Debbouche, Therm. Sci. **21**, S1 (2017).
24. Devendra Kumar, Jagdev Singh, Dumitru Baleanu, Math. Methods Appl. Sci. **40**, 5642 (2017).
25. K.M. Saad, E.H. AL-Shareef, Mohamed S. Mohamed, Xiao-Jun Yang, Eur. Phys. J. Plus **132**, 23 (2017).
26. M.A. El-Tawil, S.N. Huseen, Int. J. Appl. Math. Mech. **8**, 51 (2012).
27. S.N. Huseen, S.R. Grace, M.A. El-Tawil, Int. J. Comput. Technol. **11**, 2859 (2013).
28. O.S. Iyiola, Asian J. Curr. Eng. Math. **2**, 283 (2013).
29. S.-J. Liao, *The proposed homotopy analysis technique for the solution of nonlinear problems*, PhD thesis, Shanghai Jiao Tong University (1992).
30. S.-J. Liao, *Beyond perturbation: introduction to the homotopy analysis method* (Chapman and Hall/CRC Press, Boca Raton, 2003).
31. S.-J. Liao, Appl. Math. Comput. **147**, 499 (2004).
32. S.-J. Liao, Appl. Math. Comput. **169**, 1186 (2005).
33. Mohamed S. Mohamed, Yasser S. Hamed, Results Phys. **6**, 20 (2016).
34. K.M. Saad, A.A. AL-Shomrani, J. Fractional Calculus Appl. **7**, 61 (2016).
35. D. Baleanu, A. Atangana, Therm. Sci. **20**, 763 (2016).
36. I. Koca, A. Atangana, Chaos, Solitons Fractals **89**, 447 (2016).
37. S. Abbasbandy, M. Jalili, Numer. Algorithms **64**, 593 (2013).
38. S. Abbasbandy, E. Shivanian, Commun. Nonlinear Sci. Numer. Simulat. **16**, 2456 (2011).
39. S.M. Abo-Dahab, Mohamed S. Mohamed, T.A. Nofal, Abstr. Appl. Anal. **2013**, 614874 (2013).
40. M. Ghanbari, S. Abbasbandy, T. Allahviranloo, Appl. Comput. Math. **12**, 355 (2013).
41. M.A. Gondal, A.S. Arife, M. Khan, I. Hussain, World Appl. Sci. J. **14**, 1786 (2011).
42. S.-J. Liao, Commun. Nonlinear Sci. Numer. Simul. **15**, 2003 (2010).
43. J. Singh, D. Kumar, R. Swroop, Alex. Eng. J. **55**, 1753 (2016).
44. J. Singh, D. Kumar, R. Swroop, S. Kumar, Neural Comput. Appl. (2017) https://doi.org/10.1007/s00521-017-2909-8.
45. H.M. Srivastava, D. Kumar, J. Singh, Appl. Math. Model. **45**, 192 (2017).
46. M. Yamashita, K. Yabushita, K. Tsuboi, J. Phys. A **40**, 8403 (2007).